HHS Public Access

Author manuscript

Dev Neurobiol. Author manuscript; available in PMC 2018 March 01.

Published in final edited form as:

Dev Neurobiol. 2017 March ; 77(3): 373–389. doi:10.1002/dneu.22456.

Anatomical and Functional Neuroimaging in Awake, Behaving Marmosets

Afonso C. Silva, Ph.D.[1,*]

[1]Cerebral Microcirculation Section, Laboratory of Functional and Molecular Imaging, National Institute of Neurological Disorders and Stroke, National Institutes of Health, Bethesda, MD 20892 USA

Abstract

The common marmoset (Callithrix jacchus) is a small New World monkey that has gained significant recent interest in neuroscience research, due in great part for its compatibility with gene editing techniques, but also due to its tremendous versatility as an experimental animal model. Neuroimaging modalities, including anatomical (MRI) and functional magnetic resonance imaging (fMRI), complemented by two-photon laser scanning microscopy and electrophysiology, have been at the forefront of unraveling the anatomical and functional organization of the marmoset brain. High resolution anatomical MRI of the marmoset brain can be obtained with remarkable cytoarchitectonic detail. Functional MRI of the marmoset brain has been used to study various sensory systems, including somatosensory, auditory and visual pathways, while resting-state fMRI studies have unraveled functional brain networks that bear great correspondence to those previously described in humans. Two-photon laser scanning microscopy of the marmoset brain has enabled the simultaneous recording of neuronal activity from thousands of neurons with single cell spatial resolution. In this article, we aim to review the main results obtained by our group and our colleagues in applying neuroimaging techniques to study the marmoset brain.

Introduction

The common marmoset (Callithrix jacchus) is a small New World monkey (Haig, 1999) that is increasingly being used in the laboratory setting (Abbott et al., 2003; Mansfield, 2003), and that has gained significant recent interest in neuroscience research, due in great part for its compatibility with gene editing techniques (Okano et al., 2012; Izpisua Belmonte et al., 2015; Huang et al., 2016). Marmosets serve as an important model in the pharmaceutical industry (Smith et al., 2001) for drug and vaccine development (Gaspar et al., 1992), as well as for toxicology studies (Smith et al., 2001; Zuhlke and Weinbauer, 2003). Common research applied to marmosets range from studies of reproduction (Einspanier et al., 2006; Tardif et al., 2008), to the ethology of animal behavior (Stevenson, 1977; Saito, 2015), to the psychology of fear and anxiety (Barros et al., 2000; Kato et al., 2014), to sensory brain function (Bendor and Wang, 2005; Wang et al., 2005; Reser et al., 2009; Mitchell et al.,

Corresponding Author: Afonso C. Silva, Ph.D., Chief, Cerebral Microcirculation Section, Laboratory of Functional and Molecular Imaging, National Institute of Neurological Disorder and Stroke, National Institutes of Health, 49 Convent Drive MSC 4478, Bldg. 49 Room 3A72, Bethesda MD 20892-4478, Tel: +1-301-402-9703, Fax: +1-301-480-8670, SilvaA@ninds.nih.gov.

2014; Solomon and Rosa, 2014; Mitchell and Leopold, 2015; Miller et al., 2016). As a laboratory animal, the marmoset has a number of distinct advantages, such as small size, easy adaptation to life in captivity, trivial husbandry requirements, and prolific breeding, over the larger but more commonly used Old World primate species, the macaque (Layne and Power, 2003). Like rodents, marmosets are lissencephalic, a feature that confers the advantage of making sensorimotor, visual and auditory cortical areas easily mapped by neuroimaging and accessible to electrophysiology. Like humans, the brain of marmosets have a large amount of white matter, a feature that may confer significant advantages to marmosets as a translational model of brain disease, including multiple sclerosis (Uccelli et al., 2003; Boretius et al., 2006; t Hart et al., 2006; Helms et al., 2013; Gaitan et al., 2014; Maggi et al., 2014; Kap et al., 2016), stroke (Marshall et al., 2003; Virley et al., 2004; Bihel et al., 2010; Teo and Bourne, 2014; Puentes et al., 2015), Parkinson's disease (Hikishima et al., 2015; Yun et al., 2015; Franke et al., 2016) and Alzheimer's disease (Maclean et al., 2000). Recently, transgenic marmoset lines with germline transmission have been demonstrated (Sasaki et al., 2009), opening up novel approaches to understanding neuronal circuitry and function in the primate brain, and to make significant advancements in the study of neurological and neuropsychiatric disorders (Okano et al., 2012; Izpisua Belmonte et al., 2015; Huang et al., 2016). Thus the marmoset is poised to become increasingly important in studies in neuroscience, neurophysiology and neuropathology, with a large promise to our quest to obtain a better understanding of the physiology and pathology of the human brain.

Neuroimaging modalities including anatomical (MRI) and functional magnetic resonance imaging (fMRI), complemented by optical imaging methods including two-photon laser scanning microscopy and electrophysiology, have been at the forefront of unraveling the anatomical and functional organization of the marmoset brain – for a recent review, see (Huang et al., 2016). In this article, we aim to review the main results obtained by our group and our colleagues in applying neuroimaging techniques to study the marmoset brain. We aim to show that high resolution anatomical MRI of the marmoset brain can be obtained with remarkable cytoarchitectonic detail, while fMRI can be used to study various sensory systems, including somatosensory, auditory and visual pathways. Furthermore, MRI can be used for surgical planning and to guide the placement of tracers or neurotoxins into specific regions of the marmoset brain, enabling multimodal studies and further increasing the versatility and usefulness of marmosets in biomedical research (Mundinano et al., 2016). Complimentary to MRI/fMRI, two-photon laser scanning microscopy enables the simultaneous recording of neuronal activity from thousands of neurons with single cell spatial resolution. To make the most usage of two-photon microscopy, genetically encoded calcium indicator (GECI) molecules allow the direct monitoring of neuronal activity in the living brain with single cell resolution. This ability urges for the development of transgenic marmosets expressing GECI molecules, to enable chronic in vivo monitoring of neural activity. When combined together, the practical advantages of marmosets as experimental models and the technological developments in neuroimaging techniques make marmosets an invaluable non-human primate model in neuroscience research (Okano and Mitra, 2015; Okano et al., 2015).

Anatomical MRI of the Marmoset Brain

A major advantage of marmosets is their small body size (~350–550 g), which allows them to be imaged in specialized small animal MRI scanners. These scanners feature high magnetic field strengths (7T – 11.7T) horizontal superconducting magnets with 16 – 30 cm bores which, when combined with specialized receiver RF coils, allow imaging the marmoset brain with high sensitivity and high spatial resolution (150 – 200 μm isotropic resolution). The high spatial resolution enables mapping of individual cortical and sub-cortical brain regions, even in the small-sized marmoset brain. Indeed, high resolution MRI of the marmoset brain has provided remarkable detail about its cytoarchitecture. All the MRI pulse sequences typically used to study the human brain are available to study the marmoset brain. In MRI, soft tissue contrast is obtained when the pulse sequence parameters are adjusted to differentiate between gray matter, white matter and CSF. The main parameters governing contrast in MRI are the longitudinal relaxation time constant T_1, the transverse relaxation time constant T_2, and the water (or proton) density M_0. Different tissues have different relaxation time constants and different proton densities, and manipulation of the MRI pulse sequence parameters allows enhancing contrast in one tissue versus another. In addition, MRI can be made sensitive to the rate of exchange between free protons associated with water and those bound to macromolecules. The resulting magnetization transfer (MT) image has unique contrast due to the fact that different tissues (or the same tissue in health and disease) have different relative amounts of free water and macromolecules. Tissue structure can be probed with diffusion-weighted imaging (DWI), which measures the apparent diffusion coefficient (ADC) for water in different directions. Because of tissue structure, diffusion of water, which is normally isotropic, will be restricted by cellular membranes, fiber tracts and intracellular organelles, making the diffusion of water anisotropic. The degree of anisotropy informs on tissue structure and can be used to generate color-coded maps of tissue orientation. Another way to boost tissue contrast with MRI is through the use of contrast agents. A particularly useful contrast agent for imaging the brain is the metal ion manganese – for reviews, see (Koretsky and Silva, 2004; Silva et al., 2004; Silva and Bock, 2008). Systemic treatment with $MnCl_2$ provides exquisite MRI contrast in the brain, making manganese-enhanced MRI (MEMRI) ideal for high-resolution studies of the whole brain where as many structures as possible must be delineated.

A main source of MRI contrast in the brain is myelin. Myelin produces MRI contrast based on proton density (Clark et al., 1992), T_1 (Barbier et al., 2002; Bock et al., 2009; Bock et al., 2011; Glasser and Van Essen, 2011), and T_2 (Yoshiura et al., 2000). Myelin has been widely used to understand the organization of the cortex. Myeloarchitecture, referred to as the density and arrangement of myelinated fibers that run either radially or tangentially within the cortical layers, has classically been used to parcelate the brain cortex anatomically and functionally (Campbell, 1905; Smith, 1907). While the exact reason for the presence of cortical myelination is still subject of research, presumably it speeds the conduction of signals to the input layer of areas that require fast responses, such as the primary sensory areas, as well as efferent connections from the cortex to the spinal cord (Glasser and Van Essen, 2011). Because it has a lissencephalic brain, a normal gray-to white-matter ratio that is close to that of humans, and the lowest degree of cortical folding of all the primates (Zilles

et al., 1989), there's no other primate in which the visualization of cortical myelination is so evident as the marmoset. Using a quantitative T_1 mapping sequence (Liu et al., 2011), we verified that the presence of myelin in some areas of the marmoset cortex, such as area MT, caused as much as a 15% shortening of T_1 relative to less myelinated cortical areas (Bock et al., 2009). There was also a measurable drop of about 3% in proton density of heavily myelinated cortex relative to less myelinated cortical regions (Bock et al., 2009). Using the T_1 and proton density values for highly myelinated gray matter, we optimized the parameters of a 3D T1-weighted MPRAGE sequence that allowed acquisition of the whole marmoset brain image within 51 minutes with an isotropic resolution of 150 μm (Figure 1). The contrast between gray and white matter seen in the images in Fig. 1 is significantly higher because we optimized the imaging sequence parameters to highlight the subtle myelin-induced T_1 differences within cortical areas. The resulting increased contrast in the T1-weighted MRI highlighted myelin-rich cortical areas, as verified by post-mortem histology (Bock et al., 2009). Three primary sensory areas are easily identified in the T1-weighted image: the primary auditory cortex (A1), the primary somatosensory cortex (S1), and the primary visual cortex (V1). In addition, the middle temporal (MT) and dorsomedial (DM) visual areas are visible as well.

A better visualization of the cortical myeloarchitecture is obtained when the MRI images are shown as 3D-rendered surfaces, as if we were directly looking at the brain (Fig. 2A). Indeed, this is the best way to view the marmoset brain free of distortions. The map can be seen from any desired rotation angle, which is a useful feature when areas of the cortex are obscured. For example, Fig. 2B shows a view centered on the occipital cortex that shows both the occipital cortical surface as well as its extension into the calcarine fissure. In addition, the map can also be digitally flattened to show the entire cortex in a single 2D image (Fig. 2C). The highly myelinated areas are many. In the occipital cortex, V1 is very rich in myelin, present mainly in the stria of Gennari, which encompasses all of V1 and ends abruptly at the border of V1 with the secondary visual cortex (V2). Because the density of myelin in V2 is far lower than in V1, a clear border between both regions is well delineated and easy to identify. Note that in the flattened map of Fig. 2C, the entire extent of V1 over the occipital cortex is not shown due to difficulties flattening the calcarine fissure without introducing widespread distortions in the rest of the cortex.

Interestingly, while the myelination in V1 is almost exclusively confined to the stria of Gennari in cortical layer IV, that region was one of the first cortical areas to be segregated based on its high myelin content (Gennari, 1782). Using MEMRI, we were previously able to visualize the stripe of Gennari in the marmoset visual cortex (Bock et al., 2009). Fractionated injections of manganese (Bock et al., 2008) caused a decrease in T_1 of 35% in the V1 cortex, and of 28% in V2, respectively (Bock et al., 2009). This differential decrease in T_1 was sufficient to allow detection of the V1/V2 border on strongly T_1-weighted images, showing that MEMRI is a powerful technique for studying marmoset neuroanatomy in vivo.

Within V1, the foveal region is very densely myelinated and, from that region, two main tracts connect V1 to the two other major extrastriate visual areas that enhance well in the T_1-weighted images: area MT, readily identified by its kidney-like shape, and area DM. The exact shape of area DM is difficult to define, due to a continuous gradient of enhancement in

the region. The fundus of the superior temporal area (FST) is located ventrally and anteriorly to MT. In between DM and MT, a low myelin region named the ventral posterior parietal cortex (PPv) can be clearly identified. Area A1 can be seen in the dorsal temporal cortex and in the lateral bank of the lateral sulcus, along with the rostral auditory area (R).

As shown in Fig. 2C, the primary sensory region S1 is seen in the parietal cortex, with 3 main areas of myelination, separated by 2 lightly myelinated septa (Krubitzer and Kaas, 1990). The most medial area corresponds to the foot representation, the medial area is the hand representation, and the most lateral area of myelination corresponds to the face somatotopic representation. The secondary somatosensory cortex S2 can be seen within the medial wall of the lateral sulcus, and continuous with the parietal ventral area (PV), which is also myelinated (Krubitzer and Kaas, 1990). Adjacent to S1, the primary motor cortex M1 can be seen because of its contrast with the more heavily myelinated sensory area on the caudal border, and the relatively light myelination of the rest of the frontal cortex in its rostral border. And anterior and dorsal to M1 is area 12, located in the dorsolateral and orbital frontal cortex, which is an area that is well myelinated and of easy identification in the myeloarchitecture map. This area is an important source of projections to area MT (Burman et al., 2006).

The 3D T_1-weighted MRI of the marmoset brain allows the visualization of cortical myeloarchitecture over the entire cerebral cortex. The ability to detect cortical areas based on their myelin content in the intact brain in vivo with high spatial resolution opens up new avenues in anatomical and functional studies of the cortex. One particular interest has been in developing image-based atlases of the marmoset brain (Newman et al., 2009; Hikishima et al., 2011; Hikishima et al., 2013) to support the ever-growing use of marmosets in neuroscience research. In our 2009 publication, we presented a combined histological and MRI-based atlas of the marmoset brain to serve as a reference for studies in contemporary neuroscience research (Newman et al., 2009). In 2011, Hikishima and colleagues in Japan presented a population-averaged standard template of the common marmoset brain that was based on anatomical T_1-weighted images from 22 young adult marmosets with a high-resolution isotropic voxel size of 200 μm (Hikishima et al., 2011). They found no differences in the average brain volume and surface area between males and females, and produced tissue-segmented brain templates for gray matter, white matter and cerebral-spinal fluid (CSF). Accordingly, they found a very small mean error of 0.25 mm between the population average template and the normalized variation of distances of individual monkeys, showing that size differences between individual marmoset brains is small, as was the mean distance between the separate templates created for male versus female brains (0.26 mm) (Hikishima et al., 2011). The 3D anatomical MRI also allowed study of the early developmental stages of the marmoset brain from gestational week 8 through birth, and provided unique insight into the development of the central nervous system (CNS) in the marmoset (Hikishima et al., 2013). The development of this 3D and non-invasive anatomical imaging toolkit to study the brain is expected to be particularly useful in understanding the different phases of brain development and enable detection and evaluation of abnormal brain development in the surging transgenic marmoset models of neuropsychiatric and neurological disorders (Okano et al., 2012).

Functional MRI of the Marmoset Brain

Functional magnetic resonance imaging (fMRI) has made a remarkable impact on neuroscience research, and today fMRI is a main research tool in cognitive neuroscience (Poldrack and Farah, 2015) and showing great promise in translational and clinical studies (Bullmore, 2012; Lake et al., 2016). fMRI and other functional neuroimaging modalities, such as two-photon microscopy, are being more and more applied to study the marmoset brain. The first fMRI studies in marmosets were published in 2001 by Ferris and colleagues, who used fMRI in male marmosets to identify brain regions associated with sexual arousal (Ferris et al., 2001; Ferris et al., 2004). fMRI was also used to understand the mechanisms of corticothalamic activation during generalized absence status epilepticus (Tenney et al., 2004) and for studying the neuronal circuits responding to exposure to the psychostimulant drug MDMA (Brevard et al., 2006; Meyer et al., 2006). The above studies were conducted in conscious marmosets that were initially sedated with (dex-)medetomidine, placed in an MRI-compatible head and body restraint apparatus and, once securely restrained, awakened by reversing the anesthesia with atipamezole. Because animals are inherently noncompliant, most fMRI performed to date have required the use of anesthesia, which interferes with brain function and compromises interpretability and applicability of results. Thus, anesthesia is a major confound in any functional neuroimaging experiment. It is well known that anesthesia has a deep impact on the physiological state of the brain (Angel and Unwin, 1969), and therefore on many aspects of neurovascular coupling, including spatial localization, temporal evolution, and in the expression, dynamics and mechanism of action of the neurochemical mediators of functional hyperemia (Shapiro et al., 1978; Gerrits et al., 2001; Peeters et al., 2001; Austin et al., 2005).

In marmosets, all major sensory systems, including somatosensory, auditory and visual pathways, are amenable to be studied with fMRI. This is owing to the fact that the lissencephalic surface makes localization and visualization of the functional areas of the cortex trivial, as evident in the myeloarchitecture maps shown in Figure 2. To eliminate the use of anesthesia altogether from our fMRI experiments, we devised a training protocol to properly acclimate the marmosets to lie in the sphinx position in the MRI (Silva et al., 2011), and we designed custom-fit plastic helmets to hold their heads still, but in a comfortable and entirely non-invasive manner. The helmets were also beneficial in allowing RF coils to be built inside their inner surface, thus permitting the data to be collected with optimal sensitivity (Papoti et al., 2013).

Our first fMRI experiments aimed to better understand the activation of the somatosensory pathway and to compare both cortical and sub-cortical responses in conscious animals against those obtained in animals anesthetized under two different anesthetic regimens (Liu et al., 2013). The marmosets were equipped with contact electrodes wrapped around their wrists or ankles, and the stimulation parameters, which consisted of short (2 – 4 s) blocks of brief (0.3–0.4 ms) pulses of electrical current (1.5 – 3.0 mA) delivered with repetition frequencies of 1 Hz – 125 Hz, were adjusted to yield optimized functional responses. Figure 3 shows the areas that activate upon electrical stimulation of the wrists. The conscious animals exhibited robust fMRI activation in both contralateral and ipsilateral areas of the thalamus (not shown in Fig. 3), in addition to both ipsilateral and contralateral S1 and S2

cortices, and the caudate nucleus (Fig. 3). This pathway of functional activation is consistent with previous anatomical studies that show that, in marmosets, the thalamus projects densely and in parallel (Rowe et al., 1996) to both S1 and S2 regions (Krubitzer and Kaas, 1990; Krubitzer and Kaas, 1992) (Krubitzer and Kaas, 1992). The bilateral activation of S1 and S2 is typically observed in human fMRI experiments that employ electrical stimulation of the median nerve (Groschel et al., 2013). However, the ipsilateral activation of SI in humans is usually negative, rather than positive. Another interesting observation in marmosets is the ipsilateral activation of the thalamus. Most likely, the ipsilateral thalamic activation comes from feedback activation of ipsilateral S1 and S2 via reciprocal corticothalamic connections (Krubitzer and Kaas, 1992). When comparing the BOLD responses obtained in awake marmosets against those obtained in animals anesthetized under two different regimens of propofol anesthesia, we observed a significant attenuation of the responses in thalamus, S1, and S2, and a complete abolishment of the responses in caudate and ipsilateral S1 (Liu et al., 2013). The abolishment of the response in ipsilateral S1 but not S2 is consistent with neuronal tracing studies that show sparse interhemispheric callosal projections between ipsilateral and contralateral S1, but rich and dense direct interhemispheric projections between the two S2 (Krubitzer and Kaas, 1990).

Figure 4 shows how the fMRI responses to somatosensory stimulation relate to the cortical myeloarchitecture maps described in the previous section. Functional activation maps obtained when the stimuli were delivered to the marmoset's ankle (top row) or wrist (bottom row) are overlaid onto anatomical coronal T_1 maps. The T_1 maps are sensitive to the amount of myelin in the cortex and in white matter. Areas heavily myelinated appear darker in the T_1 maps because of their shorter T_1. The inset of Figure 4 shows the myeloarchitecture flattened cortical map (as in Fig. 2C). As mentioned in the section above, in S1 there are 3 main areas of heavy cortical myelination, which correspond to the foot (Fig. 4, inset, blue circle), the hand (Fig. 4, inset, yellow circle) and the face somatotopic representations of the body. In the coronal T_1 maps these 3 areas are indicated by cyan contours. When the animal's foot is stimulated (Fig. 4, top row), the main areas of activation in S1, pointed to by blue arrows, are located near midline, at the expected foot representation of S1 (Krubitzer and Kaas, 1990), which is indicated by the blue circle in the myeloarchitecture map (Fig. 4, inset). There's strong activation of S2 as well. Switching the stimulation to the hand (Fig. 4, bottom row) causes a lateral shift of the main areas of activation in S1 to the expected hand somatotopic representation (Krubitzer and Kaas, 1990), which is indicated by the yellow circle in the myeloarchitecture map (Fig. 4, inset). However, there's no shift in the location of activation in S2 between stimulation of the foot and of the hand. In S1, the areas of functional activation measured with fMRI localize very well within the respective myelinated areas obtained with either the T_1 maps or the T_1-weighted MPRAGE MRI.

Another primary sensory system amenable of being studied in marmosets with fMRI is the auditory system. Like humans, marmosets are a social species that utilizes a vast array of vocalizations to communicate within their groups and with other species. In addition, marmosets utilize auditory signals to navigate through and form perceptions of their environment. While auditory processing in common marmosets has been extensively studied with electrophysiology (Bendor and Wang, 2005; Wang et al., 2005), the use of non-invasive imaging techniques allows the simultaneous investigation of the multiple brain areas

involved in the perception, interpretation and generation of sounds. fMRI responses to auditory stimuli have been recently measured in marmosets from the marmosets to auditory stimuli (Sadagopan et al., 2015). Using a sparse imaging paradigm at 7T, Sadagopan and colleagues reported the existence of a caudal-rostral gradient for the processing of conspecific vocalizations in marmoset auditory cortex, vocalization processing, with anterior temporal lobe regions located close to the temporal pole (TP) and rostro-lateral to tone-responsive cortex having the greatest selectivity for vocalizations (Sadagopan et al., 2015). These results support a similar cortical organization of the auditory pathway for vocalization processing in macaques and marmosets.

When it comes to the study of the visual system, non-human primates are the animal models of choice because they share a complex parallel and hierarchical subcortical and cortical visual system comparable to that of humans (Tsao et al., 2003; Orban et al., 2004; Rosa et al., 2005). Marmosets retain the typical functional organization of the primate brain, with specializations in the eye and brain that closely resemble those found in macaques and humans (Cheong et al., 2013; Lui et al., 2013; McDonald et al., 2014; Mitchell and Leopold, 2015; Rosa and Tweedale, 2005; Yu and Rosa, 2014). The study of the visual system in marmosets with fMRI is a little more elaborate than the study of other sensory systems. While both somatosensory and auditory functional data are usually derived from passive stimuli, to which the animal does not need to be attending to the stimulus paradigm, for visual stimulation we had to train the animals to actively attend to the stimuli. First we acclimated the animals to being restrained in the sphinx position with their heads firmly held using head posts when the animal participated in electrocorticography (ECoG) experiments, or noninvasive customized 3D-printed helmets when the animals participated in fMRI experiments. The marmosets were then trained to attend to images displayed on a screen wand to actively maintain their gaze toward visual stimuli on a display. Positive reinforcement in the form of sugary water was delivered to the animals if they maintained fixation for at least 1.5 seconds during the display of the images on the screen. We then measured functional responses to assorted categories of visual stimuli with a block design paradigm (Hung et al., 2015; Hung et al., 2015). Three of the categories were structured natural photographic images of conspecific faces, conspecific body parts, and man-made objects taken within our colony. Two other control categories of spatial and phase scrambled images were created based on the face stimuli, with the intention of preserving the low-level visual features. Lastly, there was a condition where only a fixation dot was presented throughout the block.

To examine the overall responses to visual stimuli within the marmoset brain, we contrasted the BOLD signals of the five visual stimuli conditions against the fixation point condition (Fig. 5). There was selective subcortical activation in LGN, pulvinar and superior colliculus (Fig. 5A), and widespread cortical activation throughout the occipitotemporal cortex and also in frontal areas that could be easily visualized in the surface of the brain because marmosets are lissencephalic (Fig. 5B). In an elegant study combining neural tracing and DTI-MRI, Warner and colleagues showed that the pulvinar is essential to the preservation of vision following early-life lesions to V1 (Warner et al., 2015). The BOLD fMRI time courses showed robust time-locked hemodynamic responses that peaked 4 s after stimulus onset and lasted for the duration of the stimulation (Fig. 5C). The fixation dot condition did

elicit responses in some of these areas, presumably due to a general awareness (arousal) effect; the magnitude of the response, nevertheless, was lower than those evoked by other visual conditions.

Once we analyzed the raw time courses shown in Fig. 5, we asked whether these fMRI responses were selective for individual stimulus categories. We contrasted the fMRI response magnitude between faces and objects, a common contrast used in fMRI studies in humans (Kanwisher et al., 1997) and macaques (Tsao et al., 2003). The resulting fMRI maps identified at least five circumscribed cortical regions that responded more strongly to faces than to objects (Fig. 6). We labeled these areas based on their positions within the occipitotemporal cortex, approximating a naming convention applied previously in the macaque (Moeller et al., 2008). For each patch, the position within known extrastriate areas was determined based on registration with a recently published atlas (Paxinos et al., 2012) of the marmoset brain (Fig. 6A, Fig. 6C). From anterior to posterior, these consisted of an AD (anterior dorsal) and a MD (middle dorsal) patches along STS, a PD (posterior dorsal) patch in area V4t/FST, a PV (posterior ventral) patch at the V4/TEO border, and an O (occipital) patch at the V2/V3 border. For reference in Fig. 6C, we also mark the position of face-selective area MV (middle ventral) more ventrally in TE, which was observed in the ECoG recordings but not visible in fMRI due to basal susceptibility-induced artifacts. In addition to the atlas registration, we further confirmed the anatomical location of the face patches by comparing the functional maps to a high-resolution cortical myelogram obtained previously from five other marmosets (Bock et al., 2009; Bock et al., 2011). Primary sensory areas and visual areas MT and DM showed higher myelination than other cortical areas (Fig. 6C, inset). Overlapping the face patches with the boundary drawn from cortical myelination (Fig. 6C, white dashed lines), we found that face area PD is outside and ventral to area MT, in a location consistent with the location of areas V4t and FST in the atlas (Paxinos et al., 2012) and that face area O is primarily within areas V2/V3. Fig. 6D shows BOLD fMRI signal time courses for each of the face patches. Within each patch, faces elicited higher fMRI responses, with a gradation across the other categories that differed between the patches. The fMRI time courses suggest a progression of face selectivity within the occipitotemporal pathway. Specifically, AD and MD responded almost exclusively to faces, PV and PD showed intermediate responses to bodies and objects as well, and O responded strongly to all three categories, with a small but highly significant preference for faces.

In the studies illustrated by Figs. 5–6 (Hung et al., 2015; Hung et al., 2015), we were able to systematically map high-level visual selectivity in awake, behaving marmosets, revealing multiple visual cortical regions specialized for processing faces. Although further comparative work is necessary to determine the precise areal homology between primate species, the overall arrangement of face patches found in the marmoset brain, and in particular in the occipitotemporal cortex, is akin to those previously reported in macaques and humans (Tsao et al., 2008; Lafer-Sousa and Conway, 2013). The awake marmoset model opens doors to areas of investigation that are either impossible or impractical to pursue in macaques, including mapping of the uninterrupted cortex along occipitotemporal and occipitoparietal pathways with modern multi-modal neuroimaging methods such as fMRI, electrophysiology using multi-electrode arrays, and optical imaging.

Marmosets can provide more than just multisensory functional information about the brain. For example, distinct large-scale resting-state networks (RSNs) can be derived from resting BOLD fMRI data in the brains of conscious, awake marmosets (Belcher et al., 2013; Belcher et al., 2016), and that these RSNs correspond to those frequently reported in humans and anesthetized Old World monkeys and chimpanzees (Belcher et al., 2013). In particular, we found 12 anatomically relevant networks in conscious marmosets, comprised of four visual networks, two sensorimotor networks, one basal ganglia network, one cerebellar network, and four additional networks related to higher-order cognitive processing function, including a default-mode network, a salience-like network, an orbitofrontal network, and a network map that covered the frontal pole (Belcher et al., 2013). In a subsequent study, we showed that these networks were interconnected by eight hubs of maximal functional connectivity, including: the anterior cingulate; the caudate; the putamen; the lateral septal nucleus; the thalamus; the retrosplenial cortex and the medial aspect of posterior parietal area PG; the midline visual areas A19M and DM; and areas V1/V2 (Belcher et al., 2016). Our data validates the use of the conscious marmoset model for exploring the basis of resting-state networks using behavioral, pharmacological, and lesion manipulations in conditions under which human resting-state networks are obtained, and provide a baseline platform for future investigations of the brain's network topology.

Future Directions and Conclusions

Functional MRI is a wonderful technique for allowing areal observations of functional brain activity. However, while fMRI is able to provide non-invasive images of the brain with sub-millimeter spatial resolution and superior soft tissue contrast, still, at its present spatial resolution, fMRI can barely visualize the cortical cytoarchitecture and it is certainly not yet able to resolve individual cells and capillary vessels. Complementary to fMRI, two-photon laser scanning microscopy allows direct observation of neurons, astrocytes, microglia, and microvascular blood flow in the cortex. In particular, with the development of genetically encoded calcium indicators (GECIs) (Huber et al., 2012; Petreanu et al., 2012), optical monitoring of neuronal populations tagged with fluorescent calcium-sensitive molecules using two-photon laser scanning microscopy has become an attractive way to study brain function *in vivo*. GECI molecules sense calcium influx into excitable cells, and fluoresce upon calcium binding, constituting a visible marker of cellular function and activity. One particularly useful family of GECIs to allow monitoring of neural activity in vivo are GCaMP, molecules based on a fusion of the calcium-binding protein calmodulin with the green fluorescent protein (GFP) (Akerboom et al., 2012; Broussard et al.). GCaMPs can be directly delivered to discrete areas of the brain via stereotaxic injections of recombinant adeno-associated viruses (AAV) or lentiviral vectors (Tian et al., 2009; Dana et al., 2014). These viruses are able to infect non-dividing neuronal cells with apparent low toxicity, and induce stable long-term transgene expression (Smith et al., 2000; Wallace et al., 2008). While the use of GECI molecules is well established in fruit-flies, zebrafish and mice, their use in non-human primates is still limited to only a few studies (Heider et al., 2010) (Sadakane et al., 2015).

Of all non-human primates, marmosets are the ideal species for two-photon microscopy experiments, because of their lissencephalic cortex and thin skull. In a recent publication,

Sadakane and colleagues reported their experience in using AAV vectors to deliver the GECI GCaMP6f to cortical neurons of adult common marmosets (Sadakane et al., 2015). They were able to visualize spontaneous and task-induced neuronal activity over the somatosensory cortex for more than 100 days from neurons residing up to 400 μm below the pial surface. They showed that it is possible to use two-photon microscopy to simultaneously record hundreds of neurons over a time period of several months, and to reliably detect calcium transients in dendrites and axonal buttons of cortical neurons residing in the first 2 layers of the cortex (Sadakane et al., 2015). The use of optical methods for direct visualization of neural activity in the brain of awake behaving marmosets is a major future direction that significantly boosts the value of this species to neuroscience research.

However, while the local delivery of GECI molecules to specific areas of the cortex can be successfully performed using viral vectors, there are several disadvantages to the approach. First, viral vector delivery methods are invasive, requiring surgery on each animal. Second, the viruses have an inherent tropism that produces inhomogeneous expression patterns across the infection site. Third, because it is difficult to control the amount of virus delivered to the brain, these approaches can lead to undesirably high or insufficiently low expression levels of the GECI molecules. The former occurrence can cause aberrant cell death (Tian et al., 2009), while the latter can preclude the use of two-photon microscopy to visualize neuronal activity in vivo, due to lack of sufficient sensitivity. Thus, virus-mediated transgene expression is usually limited to experiments within a restricted time window (Smith et al., 2000; Nathanson et al., 2009; Watakabe et al., 2014).

One alternative approach to virus-mediated transgene expression is to develop transgenic animal lines (Diez-Garcia et al., 2005; Atkin et al., 2009; Chen et al., 2012; Zariwala et al., 2012; Dana et al., 2014; Madisen et al., 2015). The derivation of transgenic animal models is presumably a better approach to study physiological processes, as levels of expression of the transgene are endogenously regulated in a way to avoid toxicity effects associated with the local overexpression of virus-mediated transgenes (Dana et al., 2014; Madisen et al., 2015), thus allowing the visualization and study of neuronal activity under physiological conditions. Here is another place in which marmosets are playing a pivotal role (Izpisua Belmonte et al., 2015), due in great part to the successful generation of transgenic marmosets with germline transmission of the transgene (Sasaki et al., 2009). The advantages of the marmoset’s reproductive biology in having a short gestation period, relatively short time to reach sexual maturity, and the ability to produce multiple offspring enable the generation of transgenic marmoset lines within reasonably short times (Sasaki et al., 2009).

Thus, another major future area of interest is to develop transgenic marmosets that endogenously express GECI molecules in the brain. Recently, we were able to generate five different GCaMP-expressing transgenic marmoset lines by infection of naïve embryos with lentiviral vectors (Park et al., 2016). We verified integration and expression of GCaMP molecules in different tissue samples obtained from the newborn transgenic animals, and functionality of the transgene was assessed in primary cells derived from the transgenic marmosets. Germline transmission was confirmed in embryos derived from two founder animals. The embryos were transferred to recipient females, and as of today four F1 generation infants were born. These results show that transgenic marmosets expressing

GECI molecules can be successfully generated, and substantiate the promise of these non-human primates as an invaluable animal model in neuroscience, particularly in experiments aimed at monitoring neural activity and intracellular calcium dynamics with functional confocal and multi-photon optical microscopy. Examples of such potential studies could come from the work of Jude Mitchell and David Leopold (Mitchell et al., 2014; Mitchell and Leopold, 2015), which shows that the marmoset brain bears most of the visual organizational features of other primates, including macaques, with the main advantage of allowing areal mapping of its smooth cortex with two-photon microscopy and optical imaging.

In summary, the common marmoset is an important experimental animal model for basic science and translational research, in particular in the areas of neuroscience and neurodegenerative and neuropsychiatric diseases. As a primate species, marmosets offer a number of practical advantages over other commonly used NHP in experimental biology, including small size, easy adaptation to life in captivity, trivial husbandry requirements, and prolific breeding. Because marmosets are lissencephalic, localization of brain function with modern neuroimaging techniques, including fMRI, optical imaging, and multi-electrode array electrophysiology is greatly simplified. High resolution anatomical MRI of the marmoset brain can be obtained with remarkable cytoarchitectonic detail. In particular, cortical myelin can be visualized with 3D MRI to provide myeloarchitecture maps of the major sensory pathways. These maps can be used in a number of applications, from the anatomical localization of functional areas, to their use in longitudinal studies of both morphological and functional changes that occur during development or in response to plastic cortical reorganization induced by neurodegenerative diseases or following injury. Functional MRI of the marmoset brain can used to study various sensory systems, including somatosensory, auditory and visual pathways. Resting-state functional MRI studies can be used to study functional brain networks and their relevance to whole-brain circuitry and as a possible diagnostic tool for brain disorders. Two-photon laser scanning microscopy of the marmoset brain, particularly when combined with the use of GECI molecules, will enable the simultaneous recording of neuronal activity from thousands of neurons with single cell spatial resolution. The ability to develop transgenic marmoset lines with germline transmission will enable their use for chronic in vivo monitoring of neural activity, making these animals invaluable non-human primate models in neuroscience.

Acknowledgments

This research was supported by the Intramural Research Program of the NIH, NINDS (Alan P. Koretsky, Scientific Director).

References

Abbott DH, Barnett DK, Colman RJ, Yamamoto ME, Schultz-Darken NJ. Aspects of common marmoset basic biology and life history important for biomedical research. Comp Med. 2003; 53:339–350. [PubMed: 14524409]

Akerboom J, Chen TW, Wardill TJ, Tian L, Marvin JS, Mutlu S, Calderon NC, Esposti F, Borghuis BG, Sun XR, Gordus A, Orger MB, Portugues R, Engert F, Macklin JJ, Filosa A, Aggarwal A, Kerr RA, Takagi R, Kracun S, Shigetomi E, Khakh BS, Baier H, Lagnado L, Wang SS, Bargmann CI, Kimmel BE, Jayaraman V, Svoboda K, Kim DS, Schreiter ER, Looger LL. Optimization of a

GCaMP calcium indicator for neural activity imaging. J Neurosci. 2012; 32:13819–13840. [PubMed: 23035093]

Angel A, Unwin J. The effect of anaesthesia on the somatosensory cortex of the rat. J Physiol. 1969; 205:25P–26P.

Atkin SD, Patel S, Kocharyan A, Holtzclaw LA, Weerth SH, Schram V, Pickel J, Russell JT. Transgenic mice expressing a cameleon fluorescent Ca2+ indicator in astrocytes and Schwann cells allow study of glial cell Ca2+ signals in situ and in vivo. J Neurosci Methods. 2009; 181:212–226. [PubMed: 19454294]

Austin VC, Blamire AM, Allers KA, Sharp T, Styles P, Matthews PM, Sibson NR. Confounding effects of anesthesia on functional activation in rodent brain: a study of halothane and alpha-chloralose anesthesia. Neuroimage. 2005; 24:92–100. [PubMed: 15588600]

Barbier EL, Marrett S, Danek A, Vortmeyer A, van Gelderen P, Duyn J, Bandettini P, Grafman J, Koretsky AP. Imaging cortical anatomy by high-resolution MR at 3.0T: detection of the stripe of Gennari in visual area 17. Magn Reson Med. 2002; 48:735–738. [PubMed: 12353293]

Barros M, Boere V, Huston JP, Tomaz C. Measuring fear and anxiety in the marmoset (Callithrix penicillata) with a novel predator confrontation model: effects of diazepam. Behav Brain Res. 2000; 108:205–211. [PubMed: 10701664]

Belcher AM, Yen CC, Notardonato L, Ross TJ, Volkow ND, Yang Y, Stein EA, Silva AC, Tomasi D. Functional Connectivity Hubs and Networks in the Awake Marmoset Brain. Front Integr Neurosci. 2016; 10:9. [PubMed: 26973476]

Belcher AM, Yen CC, Stepp H, Gu H, Lu H, Yang Y, Silva AC, Stein EA. Large-scale brain networks in the awake, truly resting marmoset monkey. J Neurosci. 2013; 33:16796–16804. [PubMed: 24133280]

Bendor D, Wang X. The neuronal representation of pitch in primate auditory cortex. Nature. 2005; 436:1161–1165. [PubMed: 16121182]

Bihel E, Pro-Sistiaga P, Letourneur A, Toutain J, Saulnier R, Insausti R, Bernaudin M, Roussel S, Touzani O. Permanent or transient chronic ischemic stroke in the non-human primate: behavioral, neuroimaging, histological, and immunohistochemical investigations. J Cereb Blood Flow Metab. 2010; 30:273–285. [PubMed: 19794396]

Bock NA, Hashim E, Kocharyan A, Silva AC. Visualizing myeloarchitecture with magnetic resonance imaging in primates. Ann N Y Acad Sci. 2011; 1225(Suppl 1):E171–181. [PubMed: 21599695]

Bock NA, Kocharyan A, Liu JV, Silva AC. Visualizing the entire cortical myelination pattern in marmosets with magnetic resonance imaging. J Neurosci Methods. 2009; 185:15–22. [PubMed: 19737577]

Bock NA, Kocharyan A, Silva AC. Manganese-enhanced MRI visualizes V1 in the non-human primate visual cortex. NMR Biomed. 2009; 22:730–736. [PubMed: 19322808]

Bock NA, Paiva FF, Silva AC. Fractionated manganese-enhanced MRI. NMR Biomed. 2008; 21:473–478. [PubMed: 17944008]

Boretius S, Schmelting B, Watanabe T, Merkler D, Tammer R, Czeh B, Michaelis T, Frahm J, Fuchs E. Monitoring of EAE onset and progression in the common marmoset monkey by sequential high-resolution 3D MRI. NMR Biomed. 2006; 19:41–49. [PubMed: 16408325]

Brevard ME, Meyer JS, Harder JA, Ferris CF. Imaging brain activity in conscious monkeys following oral MDMA (“ecstasy”). Magn Reson Imaging. 2006; 24:707–714. [PubMed: 16824965]

Broussard GJ, Liang R, Tian L. Monitoring activity in neural circuits with genetically encoded indicators. Front Mol Neurosci. 2014; 7:97. [PubMed: 25538558]

Bullmore E. The future of functional MRI in clinical medicine. Neuroimage. 2012; 62:1267–1271. [PubMed: 22261374]

Burman KJ, Palmer SM, Gamberini M, Rosa MG. Cytoarchitectonic subdivisions of the dorsolateral frontal cortex of the marmoset monkey (Callithrix jacchus), and their projections to dorsal visual areas. J Comp Neurol. 2006; 495:149–172. [PubMed: 16435289]

Campbell, AW. Histological studies on the localisation of cerebral function. Cambridge: University Press; 1905. p. xixp. 360

Chen Q, Cichon J, Wang W, Qiu L, Lee SJ, Campbell NR, Destefino N, Goard MJ, Fu Z, Yasuda R, Looger LL, Arenkiel BR, Gan WB, Feng G. Imaging neural activity using Thy1-GCaMP transgenic mice. Neuron. 2012; 76:297–308. [PubMed: 23083733]

Clark VP, Courchesne E, Grafe M. In vivo myeloarchitectonic analysis of human striate and extrastriate cortex using magnetic resonance imaging. Cereb Cortex. 1992; 2:417–424. [PubMed: 1422094]

Dana H, Chen TW, Hu A, Shields BC, Guo C, Looger LL, Kim DS, Svoboda K. Thy1-GCaMP6 transgenic mice for neuronal population imaging in vivo. PLoS One. 2014; 9:e108697. [PubMed: 25250714]

Diez-Garcia J, Matsushita S, Mutoh H, Nakai J, Ohkura M, Yokoyama J, Dimitrov D, Knopfel T. Activation of cerebellar parallel fibers monitored in transgenic mice expressing a fluorescent Ca2+ indicator protein. Eur J Neurosci. 2005; 22:627–635. [PubMed: 16101744]

Einspanier A, Lieder K, Einspanier R, Husen B. The common marmoset monkey as a model for implantation and early pregnancy research. Methods Mol Med. 2006; 121:111–121. [PubMed: 16251739]

Ferris CF, Snowdon CT, King JA, Duong TQ, Ziegler TE, Ugurbil K, Ludwig R, Schultz-Darken NJ, Wu Z, Olson DP, Sullivan JM Jr, Tannenbaum PL, Vaughan JT. Functional imaging of brain activity in conscious monkeys responding to sexually arousing cues. Neuroreport. 2001; 12:2231–2236. [PubMed: 11447340]

Ferris CF, Snowdon CT, King JA, Sullivan JM Jr, Ziegler TE, Olson DP, Schultz-Darken NJ, Tannenbaum PL, Ludwig R, Wu Z, Einspanier A, Vaughan JT, Duong TQ. Activation of neural pathways associated with sexual arousal in non-human primates. J Magn Reson Imaging. 2004; 19:168–175. [PubMed: 14745749]

Franke SK, van Kesteren RE, Hofman S, Wubben JA, Smit AB, Philippens IH. Individual and Familial Susceptibility to MPTP in a Common Marmoset Model for Parkinson's Disease. Neurodegener Dis. 2016

Gaitan MI, Maggi P, Wohler J, Leibovitch E, Sati P, Calandri IL, Merkle H, Massacesi L, Silva AC, Jacobson S, Reich DS. Perivenular brain lesions in a primate multiple sclerosis model at 7-tesla magnetic resonance imaging. Mult Scler. 2014; 20:64–71. [PubMed: 23773983]

Gaspar AM, Vitral CL, Marchevsky RS, Yoshida CF, Schatzmayr HG. A Brazilian hepatitis A virus isolated and adapted in primate and primate cell line as a chance for the development of a vaccine. Mem Inst Oswaldo Cruz. 1992; 87:449–450. [PubMed: 1343657]

Gennari, F. Ex regio typographeo. Parma: 1782. De peculiari structura cerebri nonnullisque eius morbis.

Gerrits RJ, Stein EA, Greene AS. Anesthesia alters NO-mediated functional hyperemia. Brain Res. 2001; 907:20–26. [PubMed: 11430881]

Glasser MF, Van Essen DC. Mapping human cortical areas in vivo based on myelin content as revealed by T1- and T2-weighted MRI. J Neurosci. 2011; 31:11597–11616. [PubMed: 21832190]

Groschel S, Sohns JM, Schmidt-Samoa C, Baudewig J, Becker L, Dechent P, Kastrup A. Effects of age on negative BOLD signal changes in the primary somatosensory cortex. Neuroimage. 2013; 71:10–18. [PubMed: 23296182]

Haig D. What is a marmoset? Am J Primatol. 1999; 49:285–296. [PubMed: 10553958]

Helms G, Garea-Rodriguez E, Schlumbohm C, Konig J, Dechent P, Fuchs E, Wilke M. Structural and quantitative neuroimaging of the common marmoset monkey using a clinical MRI system. J Neurosci Methods. 2013; 215:121–131. [PubMed: 23473795]

Hikishima K, Ando K, Yano R, Kawai K, Komaki Y, Inoue T, Itoh T, Yamada M, Momoshima S, Okano HJ, Okano H. Parkinson Disease: Diffusion MR Imaging to Detect Nigrostriatal Pathway Loss in a Marmoset Model Treated with 1-Methyl-4-phenyl-1,2,3,6-tetrahydropyridine. Radiology. 2015; 275:430–437. [PubMed: 25602507]

Hikishima K, Quallo MM, Komaki Y, Yamada M, Kawai K, Momoshima S, Okano HJ, Sasaki E, Tamaoki N, Lemon RN, Iriki A, Okano H. Population-averaged standard template brain atlas for the common marmoset (Callithrix jacchus). Neuroimage. 2011; 54:2741–2749. [PubMed: 21044887]

Hikishima K, Sawada K, Murayama AY, Komaki Y, Kawai K, Sato N, Inoue T, Itoh T, Momoshima S, Iriki A, Okano HJ, Sasaki E, Okano H. Atlas of the developing brain of the marmoset monkey constructed using magnetic resonance histology. Neuroscience. 2013; 230:102–113. [PubMed: 23047019]

Huang L, Merson TD, Bourne JA. In vivo whole brain, cellular and molecular imaging in nonhuman primate models of neuropathology. Neurosci Biobehav Rev. 2016; 66:104–118. [PubMed: 27151822]

Huber D, Gutnisky DA, Peron S, O'Connor DH, Wiegert JS, Tian L, Oertner TG, Looger LL, Svoboda K. Multiple dynamic representations in the motor cortex during sensorimotor learning. Nature. 2012; 484:473–478. [PubMed: 22538608]

Hung CC, Yen CC, Ciuchta JL, Papoti D, Bock NA, Leopold DA, Silva AC. Functional mapping of face-selective regions in the extrastriate visual cortex of the marmoset. J Neurosci. 2015; 35:1160–1172. [PubMed: 25609630]

Hung CC, Yen CC, Ciuchta JL, Papoti D, Bock NA, Leopold DA, Silva AC. Functional MRI of visual responses in the awake, behaving marmoset. Neuroimage. 2015; 120:1–11. [PubMed: 26149609]

Izpisua Belmonte JC, Callaway EM, Caddick SJ, Churchland P, Feng G, Homanics GE, Lee KF, Leopold DA, Miller CT, Mitchell JF, Mitalipov S, Moutri AR, Movshon JA, Okano H, Reynolds JH, Ringach D, Sejnowski TJ, Silva AC, Strick PL, Wu J, Zhang F. Brains, genes, and primates. Neuron. 2015; 86:617–631. [PubMed: 25950631]

Kanwisher N, McDermott J, Chun MM. The fusiform face area: a module in human extrastriate cortex specialized for face perception. J Neurosci. 1997; 17:4302–4311. [PubMed: 9151747]

Kap YS, Jagessar SA, Dunham Jt, Hart BA. The common marmoset as an indispensable animal model for immunotherapy development in multiple sclerosis. Drug Discov Today. 2016

Kato Y, Gokan H, Oh-Nishi A, Suhara T, Watanabe S, Minamimoto T. Vocalizations associated with anxiety and fear in the common marmoset (Callithrix jacchus). Behav Brain Res. 2014; 275:43–52. [PubMed: 25193318]

Koretsky AP, Silva AC. Manganese-enhanced magnetic resonance imaging (MEMRI). NMR Biomed. 2004; 17:527–531. [PubMed: 15617051]

Krubitzer LA, Kaas JH. The organization and connections of somatosensory cortex in marmosets. J Neurosci. 1990; 10:952–974. [PubMed: 2108231]

Krubitzer LA, Kaas JH. The somatosensory thalamus of monkeys: cortical connections and a redefinition of nuclei in marmosets. J Comp Neurol. 1992; 319:123–140. [PubMed: 1375605]

Lafer-Sousa R, Conway BR. Parallel, multi-stage processing of colors, faces and shapes in macaque inferior temporal cortex. Nat Neurosci. 2013; 16:1870–1878. [PubMed: 24141314]

Lake EM, Bazzigaluppi P, Stefanovic B. Functional magnetic resonance imaging in chronic ischaemic stroke. Philos Trans R Soc Lond B Biol Sci. 2016:371.

Layne DG, Power RA. Husbandry, handling, and nutrition for marmosets. Comp Med. 2003; 53:351–359. [PubMed: 14524410]

Liu JV, Bock NA, Silva AC. Rapid high-resolution three-dimensional mapping of T1 and age-dependent variations in the non-human primate brain using magnetization-prepared rapid gradient-echo (MPRAGE) sequence. Neuroimage. 2011; 56:1154–1163. [PubMed: 21376814]

Liu JV, Hirano Y, Nascimento GC, Stefanovic B, Leopold DA, Silva AC. fMRI in the awake marmoset: somatosensory-evoked responses, functional connectivity, and comparison with propofol anesthesia. Neuroimage. 2013; 78:186–195. [PubMed: 23571417]

Maclean CJ, Baker HF, Ridley RM, Mori H. Naturally occurring and experimentally induced beta-amyloid deposits in the brains of marmosets (Callithrix jacchus). J Neural Transm (Vienna). 2000; 107:799–814. [PubMed: 11005545]

Madisen L, Garner AR, Shimaoka D, Chuong AS, Klapoetke NC, Li L, van der Bourg A, Niino Y, Egolf L, Monetti C, Gu H, Mills M, Cheng A, Tasic B, Nguyen TN, Sunkin SM, Benucci A, Nagy A, Miyawaki A, Helmchen F, Empson RM, Knopfel T, Boyden ES, Reid RC, Carandini M, Zeng H. Transgenic mice for intersectional targeting of neural sensors and effectors with high specificity and performance. Neuron. 2015; 85:942–958. [PubMed: 25741722]

Maggi P, Macri SM, Gaitan MI, Leibovitch E, Wholer JE, Knight HL, Ellis M, Wu T, Silva AC, Massacesi L, Jacobson S, Westmoreland S, Reich DS. The formation of inflammatory

demyelinated lesions in cerebral white matter. Ann Neurol. 2014; 76:594–608. [PubMed: 25088017]

Mansfield K. Marmoset models commonly used in biomedical research. Comp Med. 2003; 53:383–392. [PubMed: 14524414]

Marshall JW, Ridley RM, Baker HF, Hall LD, Carpenter TA, Wood NI. Serial MRI, functional recovery, and long-term infarct maturation in a non-human primate model of stroke. Brain Res Bull. 2003; 61:577–585. [PubMed: 14519454]

Meyer JS, Brevard ME, Piper BJ, Ali SF, Ferris CF. Neural effects of MDMA as determined by functional magnetic resonance imaging and magnetic resonance spectroscopy in awake marmoset monkeys. Ann N Y Acad Sci. 2006; 1074:365–376. [PubMed: 17105934]

Miller CT, Freiwald WA, Leopold DA, Mitchell JF, Silva AC, Wang X. Marmosets: A Neuroscientific Model of Human Social Behavior. Neuron. 2016; 90:219–233. [PubMed: 27100195]

Mitchell JF, Leopold DA. The marmoset monkey as a model for visual neuroscience. Neurosci Res. 2015; 93:20–46. [PubMed: 25683292]

Mitchell JF, Reynolds JH, Miller CT. Active vision in marmosets: a model system for visual neuroscience. J Neurosci. 2014; 34:1183–1194. [PubMed: 24453311]

Moeller S, Freiwald WA, Tsao DY. Patches with links: a unified system for processing faces in the macaque temporal lobe. Science. 2008; 320:1355–1359. [PubMed: 18535247]

Mundinano IC, Flecknell PA, Bourne JA. MRI-guided stereotaxic brain surgery in the infant and adult common marmoset. Nat Protoc. 2016; 11:1299–1308. [PubMed: 27336707]

Nathanson JL, Yanagawa Y, Obata K, Callaway EM. Preferential labeling of inhibitory and excitatory cortical neurons by endogenous tropism of adeno-associated virus and lentivirus vectors. Neuroscience. 2009; 161:441–450. [PubMed: 19318117]

Newman JD, Kenkel WM, Aronoff EC, Bock NA, Zametkin MR, Silva AC. A combined histological and MRI brain atlas of the common marmoset monkey, Callithrix jacchus. Brain Res Rev. 2009; 62:1–18. [PubMed: 19744521]

Okano H, Hikishima K, Iriki A, Sasaki E. The common marmoset as a novel animal model system for biomedical and neuroscience research applications. Semin Fetal Neonatal Med. 2012; 17:336–340. [PubMed: 22871417]

Okano H, Mitra P. Brain-mapping projects using the common marmoset. Neurosci Res. 2015; 93:3–7. [PubMed: 25264372]

Okano H, Miyawaki A, Kasai K. Brain/MINDS: brain-mapping project in Japan. Philos Trans R Soc Lond B Biol Sci. 2015:370.

Orban GA, Van Essen D, Vanduffel W. Comparative mapping of higher visual areas in monkeys and humans. Trends Cogn Sci. 2004; 8:315–324. [PubMed: 15242691]

Papoti D, Yen CC, Mackel JB, Merkle H, Silva AC. An embedded four-channel receive-only RF coil array for fMRI experiments of the somatosensory pathway in conscious awake marmosets. NMR Biomed. 2013; 26:1395–1402. [PubMed: 23696219]

Park JE, Zhang XF, Choi S-H, Okahara J, Sasaki E, Silva AC. Generation of transgenic marmosets expressing genetically encoded calcium indicators. Sci Rep. 2016

Paxinos, G., Watson, C., Petrides, M., Rosa, MG., Tokuno, H. The marmoset brain in stereotaxic coordinates. Oxford, UK: Academic Press; 2012.

Peeters RR, Tindemans I, De Schutter E, Van der Linden A. Comparing BOLD fMRI signal changes in the awake and anesthetized rat during electrical forepaw stimulation. Magn Reson Imaging. 2001; 19:821–826. [PubMed: 11551722]

Petreanu L, Gutnisky DA, Huber D, Xu NL, O'Connor DH, Tian L, Looger L, Svoboda K. Activity in motor-sensory projections reveals distributed coding in somatosensation. Nature. 2012; 489:299–303. [PubMed: 22922646]

Poldrack RA, Farah MJ. Progress and challenges in probing the human brain. Nature. 2015; 526:371–379. [PubMed: 26469048]

Puentes S, Kaido T, Hanakawa T, Ichinohe N, Otsuki T, Seki K. Internal capsule stroke in the common marmoset. Neuroscience. 2015; 284:400–411. [PubMed: 25453768]

Reser DH, Burman KJ, Richardson KE, Spitzer MW, Rosa MG. Connections of the marmoset rostrotemporal auditory area: express pathways for analysis of affective content in hearing. Eur J Neurosci. 2009; 30:578–592. [PubMed: 19663937]

Rosa MG, Palmer SM, Gamberini M, Tweedale R, Pinon MC, Bourne JA. Resolving the organization of the New World monkey third visual complex: the dorsal extrastriate cortex of the marmoset (Callithrix jacchus). J Comp Neurol. 2005; 483:164–191. [PubMed: 15678474]

Rowe MJ, Turman AB, Murray GM, Zhang HQ. Parallel organization of somatosensory cortical areas I and II for tactile processing. Clin Exp Pharmacol Physiol. 1996; 23:931–938. [PubMed: 8911737]

Sadagopan S, Temiz-Karayol NZ, Voss HU. High-field functional magnetic resonance imaging of vocalization processing in marmosets. Sci Rep. 2015; 5:10950. [PubMed: 26091254]

Sadakane O, Masamizu Y, Watakabe A, Terada S, Ohtsuka M, Takaji M, Mizukami H, Ozawa K, Kawasaki H, Matsuzaki M, Yamamori T. Long-Term Two-Photon Calcium Imaging of Neuronal Populations with Subcellular Resolution in Adult Non-human Primates. Cell Rep. 2015; 13:1989–1999. [PubMed: 26655910]

Saito A. The marmoset as a model for the study of primate parental behavior. Neurosci Res. 2015; 93:99–109. [PubMed: 25575642]

Sasaki E, Suemizu H, Shimada A, Hanazawa K, Oiwa R, Kamioka M, Tomioka I, Sotomaru Y, Hirakawa R, Eto T, Shiozawa S, Maeda T, Ito M, Ito R, Kito C, Yagihashi C, Kawai K, Miyoshi H, Tanioka Y, Tamaoki N, Habu S, Okano H, Nomura T. Generation of transgenic non-human primates with germline transmission. Nature. 2009; 459:523–527. [PubMed: 19478777]

Shapiro HM, Greenberg JH, Reivich M, Ashmead G, Sokoloff L. Local cerebral glucose uptake in awake and halothane-anesthetized primates. Anesthesiology. 1978; 48:97–103. [PubMed: 418710]

Silva AC, Bock NA. Manganese-enhanced MRI: an exceptional tool in translational neuroimaging. Schizophr Bull. 2008; 34:595–604. [PubMed: 18550591]

Silva AC, Lee JH, Aoki I, Koretsky AP. Manganese-enhanced magnetic resonance imaging (MEMRI): methodological and practical considerations. NMR Biomed. 2004; 17:532–543. [PubMed: 15617052]

Silva AC, Liu JV, Hirano Y, Leoni RF, Merkle H, Mackel JB, Zhang XF, Nascimento GC, Stefanovic B. Longitudinal functional magnetic resonance imaging in animal models. Methods Mol Biol. 2011; 711:281–302. [PubMed: 21279608]

Smith D, Trennery P, Farningham D, Klapwijk J. The selection of marmoset monkeys (Callithrix jacchus) in pharmaceutical toxicology. Lab Anim. 2001; 35:117–130. [PubMed: 11315160]

Smith GE. A New Topographical Survey of the Human Cerebral Cortex, Being an Account of the Distribution of the Anatomically Distinct Cortical Areas and Their Relationship to the Cerebral Sulci. Journal of Anatomy and Physiology. 1907; 41:237–254. [PubMed: 17232738]

Smith RL, Traul DL, Schaack J, Clayton GH, Staley KJ, Wilcox CL. Characterization of promoter function and cell-type-specific expression from viral vectors in the nervous system. J Virol. 2000; 74:11254–11261. [PubMed: 11070024]

Solomon SG, Rosa MG. A simpler primate brain: the visual system of the marmoset monkey. Front Neural Circuits. 2014; 8:96. [PubMed: 25152716]

Stevenson MF. The common marmoset (Callithrix jacchus jacchus) as a model for ethological research. Lab Anim Sci. 1977; 27:895–900. [PubMed: 413004]

t Hart BA, Smith P, Amor S, Strijkers GJ, Blezer EL. MRI-guided immunotherapy development for multiple sclerosis in a primate. Drug Discov Today. 2006; 11:58–66. [PubMed: 16478692]

Tardif SD, Araujo A, Arruda MF, French JA, Sousa MB, Yamamoto ME. Reproduction and aging in marmosets and tamarins. Interdiscip Top Gerontol. 2008; 36:29–48. [PubMed: 18523371]

Tenney JR, Marshall PC, King JA, Ferris CF. fMRI of generalized absence status epilepticus in conscious marmoset monkeys reveals corticothalamic activation. Epilepsia. 2004; 45:1240–1247. [PubMed: 15461678]

Teo L, Bourne JA. A reproducible and translatable model of focal ischemia in the visual cortex of infant and adult marmoset monkeys. Brain Pathol. 2014; 24:459–474. [PubMed: 25469561]

Tian L, Hires SA, Mao T, Huber D, Chiappe ME, Chalasani SH, Petreanu L, Akerboom J, McKinney SA, Schreiter ER, Bargmann CI, Jayaraman V, Svoboda K, Looger LL. Imaging neural activity in

worms, flies and mice with improved GCaMP calcium indicators. Nat Methods. 2009; 6:875–881. [PubMed: 19898485]

Tsao DY, Freiwald WA, Knutsen TA, Mandeville JB, Tootell RB. Faces and objects in macaque cerebral cortex. Nat Neurosci. 2003; 6:989–995. [PubMed: 12925854]

Tsao DY, Moeller S, Freiwald WA. Comparing face patch systems in macaques and humans. Proc Natl Acad Sci U S A. 2008; 105:19514–19519. [PubMed: 19033466]

Uccelli A, Giunti D, Capello E, Roccatagliata L, Mancardi GL. EAE in the common marmoset Callithrix jacchus. Int MS J. 2003; 10:6–12. [PubMed: 12906764]

Virley D, Hadingham SJ, Roberts JC, Farnfield B, Elliott H, Whelan G, Golder J, David C, Parsons AA, Hunter AJ. A new primate model of focal stroke: endothelin-1-induced middle cerebral artery occlusion and reperfusion in the common marmoset. J Cereb Blood Flow Metab. 2004; 24:24–41. [PubMed: 14688614]

Wallace DJ, Meyer zum Alten Borgloh S, Astori S, Yang Y, Bausen M, Kugler S, Palmer AE, Tsien RY, Sprengel R, Kerr JN, Denk W, Hasan MT. Single-spike detection in vitro and in vivo with a genetic Ca2+ sensor. Nat Methods. 2008; 5:797–804. [PubMed: 19160514]

Wang X, Lu T, Snider RK, Liang L. Sustained firing in auditory cortex evoked by preferred stimuli. Nature. 2005; 435:341–346. [PubMed: 15902257]

Warner CE, Kwan WC, Wright D, Johnston LA, Egan GF, Bourne JA. Preservation of vision by the pulvinar following early-life primary visual cortex lesions. Curr Biol. 2015; 25:424–434. [PubMed: 25601551]

Watakabe A, Ohtsuka M, Kinoshita M, Takaji M, Isa K, Mizukami H, Ozawa K, Isa T, Yamamori T. Comparative analyses of adeno-associated viral vector serotypes 1, 2, 5, 8 and 9 in marmoset, mouse and macaque cerebral cortex. Neurosci Res. 2014

Yoshiura T, Higano S, Rubio A, Shrier DA, Kwok WE, Iwanaga S, Numaguchi Y. Heschl and superior temporal gyri: low signal intensity of the cortex on T2-weighted MR images of the normal brain. Radiology. 2000; 214:217–221. [PubMed: 10644127]

Yun JW, Ahn JB, Kang BC. Modeling Parkinson's disease in the common marmoset (Callithrix jacchus): overview of models, methods, and animal care. Lab Anim Res. 2015; 31:155–165. [PubMed: 26755918]

Zariwala HA, Borghuis BG, Hoogland TM, Madisen L, Tian L, De Zeeuw CI, Zeng H, Looger LL, Svoboda K, Chen TW. A Cre-dependent GCaMP3 reporter mouse for neuronal imaging in vivo. J Neurosci. 2012; 32:3131–3141. [PubMed: 22378886]

Zilles K, Armstrong E, Moser KH, Schleicher A, Stephan H. Gyrification in the cerebral cortex of primates. Brain Behav Evol. 1989; 34:143–150. [PubMed: 2512000]

Zuhlke U, Weinbauer G. The common marmoset (Callithrix jacchus) as a model in toxicology. Toxicol Pathol. 2003; 31(Suppl):123–127. [PubMed: 12597440]

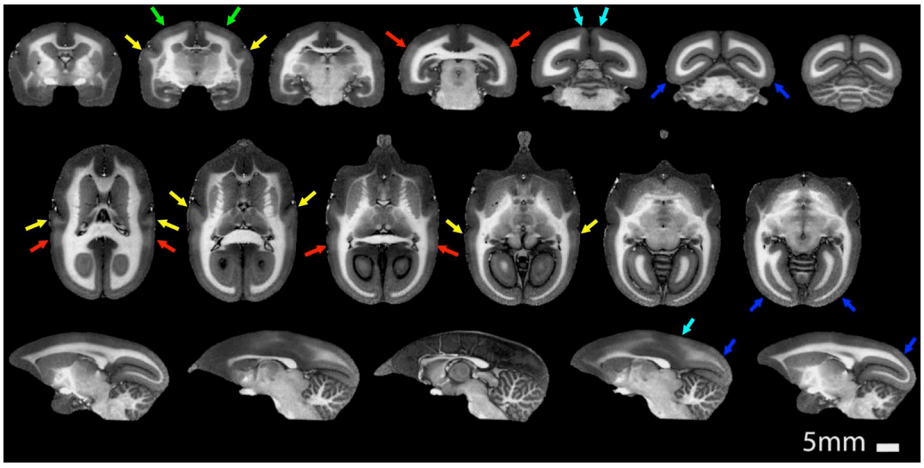

Figure 1.

Coronal (top row), axial (middle row) and sagittal (bottom row) T_1-weighted MPRAGE images of the marmoset brain acquired with a spatial resolution of 150 μm in 51 minutes. While excellent gray matter to white matter contrast can be observed, the sequence parameters were optimized to maximize contrast between heavily myelinated areas of the cortex and those that have a lower myelin content. The arrows point to heavily myelinated cortical areas: A1 (yellow), S1 (green), V1 (blue), DM (cyan), MT (red).

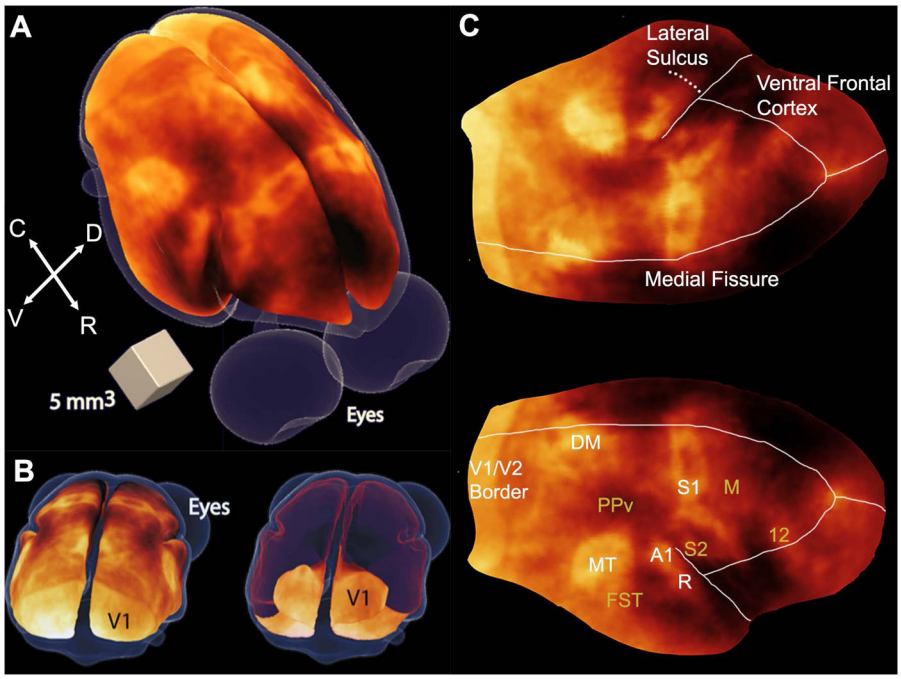

Figure 2.

Myeloarchitecture maps of the marmoset cortex. (A) 3D surface map of the cortical myeloarchitecture of the marmoset brain. Richly myelinated cortical areas appear brighter than less myelinated areas. C = caudal; R = rostral; D = dorsal; V = ventral. (B) Back (caudal) views of the 3D surface myeloarchitecture map showing the entire cortical surface (left) and showing only the calcarine fissure of V1 (right), by making the dorsal surface of the map transparent (shown in red). (C) Flattened map of the cortical myeloarchitecture. Major myelinated areas of the cortex are labeled in white, while other cortical structures are labeled in mustard: V1/V2, primary and secondary visual areas; MT, middle temporal area; DM, dorsomedial area; A1, primary auditory area; R, rostral auditory area; S1, primary somatosensory cortex; M, motor cortex including primary and premotor areas and the frontal eye fields; PPv, ventral posterior parietal cortex; FST, fundus of the superior temporal area; S2, secondary somatosensory cortex; PV, parietal ventral area; 12, area 12. Adapted from (Bock et al., 2011).

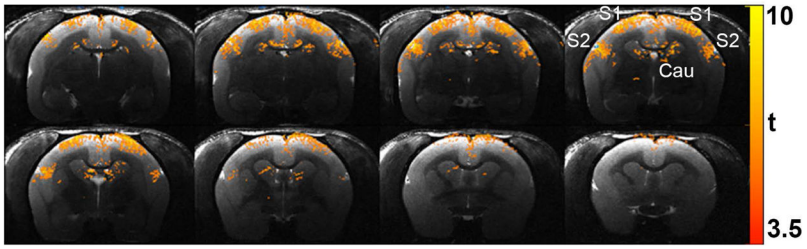

Figure 3.

Functional MRI BOLD activation maps obtained with high spatial resolution (250 × 250 × 1000 μm^3) from a conscious awake marmoset in response to bilateral somatosensory stimulation of the hands. The main areas of activation are the primary (S1) and secondary (S2) somatosensory cortices, caudate (Cau) and the thalamus (not shown). The colorbar indicates the t-values of functional activation.

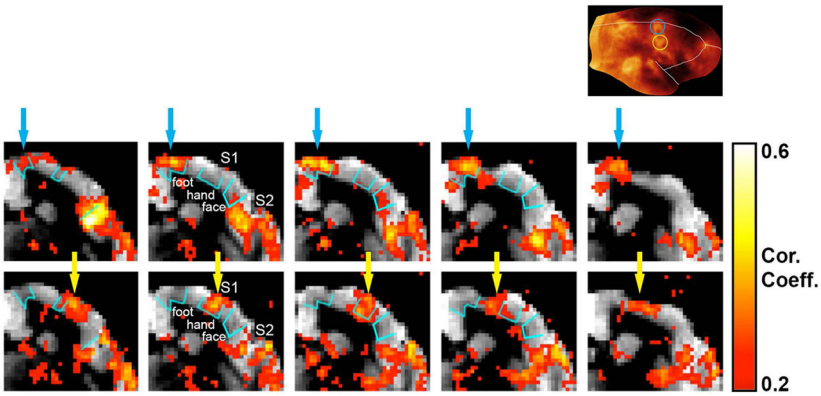

Figure 4.

Relationship between the cortical myeloarchitecture maps and the fMRI activation maps in response to somatosensory stimulation. The fMRI maps obtained during unilateral stimulation of the marmoset's ankle (top row) or wrist (bottom row) are overlaid onto anatomical coronal T_1 maps. The inset shows the myeloarchitecture flattened cortical map. The 3 main areas of heavy cortical myelination in S1, which correspond to the foot (inset, blue circle), the hand (inset, yellow circle) and the face somatotopic representations of the body, are indicated by cyan contours in the coronal T_1 maps. Stimulation of the marmoset's ankle (top row) causes activation in S1 near midline (blue arrows), at the expected foot representation of S1. Stimulation of the marmoset's wrist (bottom row) causes a lateral shift of the main areas of activation in S1 to the expected hand representation (yellow arrows). Notice strong activation of S2 to both stimulation of the ankle and the wrist.

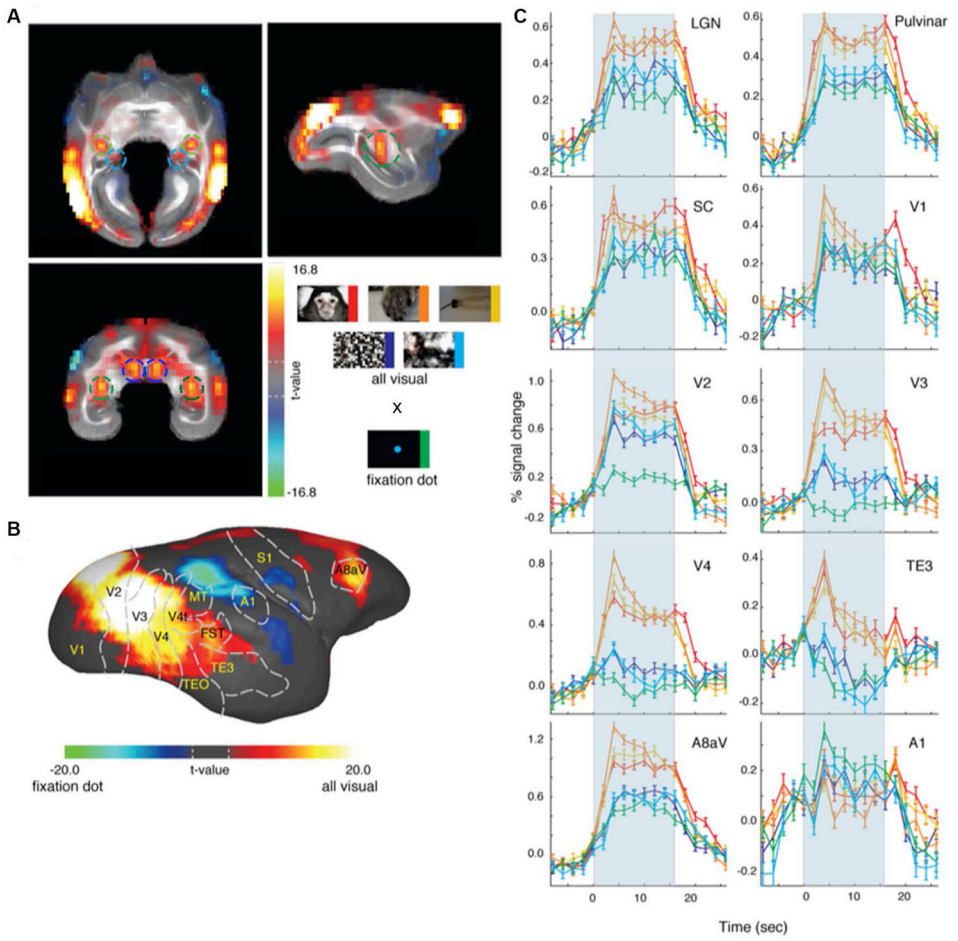

Figure 5.

Functional MRI responses of awake marmosets to visual stimulation. Visual stimuli were delivered in a block design paradigm, in which each stimulation block contained images belonging to any one of five different stimulus categories: natural photographic images of conspecific faces (red), conspecific body parts (orange); man-made objects familiar to the marmosets (yellow); spatially-scrambled images (purple) and phase-scrambled images (cyan). In addition, there was a condition where only a fixation dot was presented throughout the block (green). (A) Overall fMRI responses to visual stimuli of all five visual stimuli conditions against the fixation point condition. There was selective subcortical activation in LGN (green circles), pulvinar (cyan circles) and superior colliculus (blue circles). (B) Surface map showing widespread cortical activation throughout the occipitotemporal cortex and frontal areas in response to visual stimuli. (C) BOLD fMRI time courses showing the responses in cortical and subcortical areas to each of the different stimuli category. Adapted from (Hung et al., 2015).

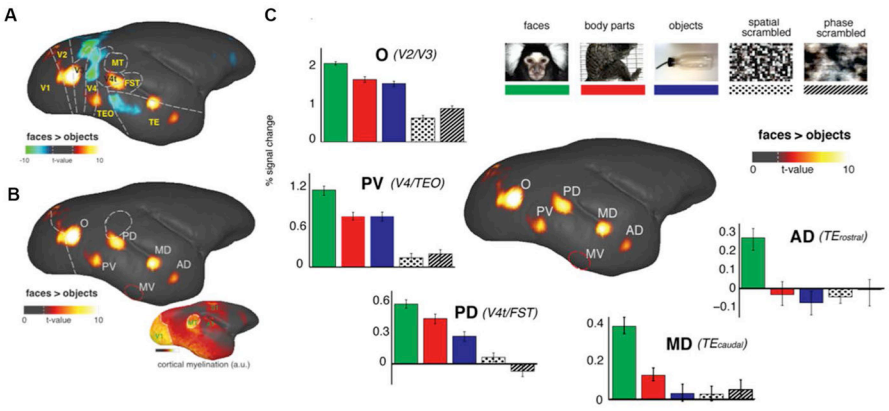

Figure 6.

Functional MRI responses of awake marmosets to visual stimulation. Visual stimuli were delivered in a block design paradigm, in which each stimulation block contained images belonging to any one of five different stimulus categories: natural photographic images of conspecific faces (green), conspecific body parts (red); man-made objects familiar to the marmosets (blue); spatially-scrambled images (dots) and phase-scrambled images (hashed). The fMRI responses to faces were contrasted against those to objects. (A) Functional map contrasting faces versus objects reveals five discrete functional areas. The colorbar represents the t value scale. Dashed line indicates the t value corresponding to a p value < 0.05 after correcting for multiple comparisons. No specific threshold was applied to the map. (B) Only the positive contrast of the faces versus objects map is shown to highlight the five face-selective areas. Top left to bottom right, face patches O (V2/V3), PV (V4/TEO), PD (V4t/FST), MD (posterior TE), and AD (anterior TE). A sixth face patch, indicated by a red circle and labeled area MV, was detected with ECoG but not with fMRI due to signal dropout. Right inset: cortical myelination strength obtained with T_1-weighted MRI from five other animals. (C) Median percentage BOLD signal changes to each stimulus category relative to the fixation dot alone condition. Within each patch, faces elicited higher fMRI responses, with a gradation across the other categories that differed between the patches. The fMRI signal changes suggest a progression of face selectivity within the occipitotemporal pathway. Specifically, AD and MD responded almost exclusively to faces, PV and PD showed intermediate responses to bodies and objects as well, and O responded strongly to all three categories, with a small but highly significant preference for faces.